What hydrogen spin measures in NGC 2403

One spin-temperature detection and four radial limits

At a disk radius of **2.62 kpc**, Braun measured an effective 21-cm spin temperature of **53 ± 15 K** in NGC 2403. This measures the relative occupations of the atomic hydrogen singlet and triplet. It supplies an observational constraint independent of fitting the galaxy's rotation curve. The continuum source is an H II region inside the galaxy. Uncertain foreground depth and beam filling affect the measurement.

Disk radius, kpc	Spin temperature	H I column, solar masses/pc²	Required Q / H I mass column
2.62	53 ± 15 K	6.85	4.20
8.49	>62 K	4.32	5.94
11.32	>63 K	2.85	7.23
13.94	>45 K	1.76	10.47
17.56	>63 K	0.73	22.18

These are all the sightlines with a spin detection or limit inside the archived rotation curve. A fifth limit, >9 K at 32.03 kpc, lies beyond it. Three additional sightlines have no spin constraint. Radii use Braun's disk-plane angles and the project distance of 3.16 Mpc. The table pairs a pencil-beam temperature with the azimuthally averaged hydrogen column and the rotation-inferred source at that radius.

How much entropy does the line measure?

Write $T_{hf} = h\nu/k_B = 0.068169$ K and $p_1/p_0 = 3\exp(-T_{hf}/T_s)$. For equal occupation of the three triplet sublevels, the entropy per atom in units of k_B is $h_{hf} = -p_0 \ln p_0 - p_1 \ln(p_1/3)$. At the detection, $p_1 = 0.749759$ and $h_{hf} = 1.38629421$. The maximum is $\ln 4 = 1.38629436$. At each of the three outer limits the fractional deficit from that maximum is below $\mathbf{1.56 \times 10^{-7}}$ in this effective-temperature calculation.

Braun's independent spectral-shape analysis gives kinetic temperatures of 87, 90, 94, 94 and 108 K in five radial zones centered between 1.76 and 15.55 kpc. These fits characterize the bright H I filament network. Identifying its kinetic and spin temperatures would give the same near-saturation. Unresolved mixtures and polarized sublevels can carry different entropy at the same reported effective temperature.

Braun, absorption measurements, Table 3 · Braun, emission-line fits, Table 3 · HALOGAS intensity maps · Laboratory measurement of the hydrogen hyperfine splitting.

Where the slower falloff enters the rotation curve

The original stationary spherical ESFD source obeys $Q_r = \beta_s s J_r/c^2 = (v^2 - v_b^2)/(4\pi G r)$. The baryonic force retains the project's disk geometry. On the 21 outer measurements, between 10.93 and 20.87 kpc, the inferred Q_r has a logarithmic slope of **−0.651**. The original inner exponential gives **−0.922** on those same radii. Across the span of the three outer absorption sightlines, that slope difference corresponds to a **12.6%** relative change. The measured level-population entropy per atom has too little temperature dependence to account for it.

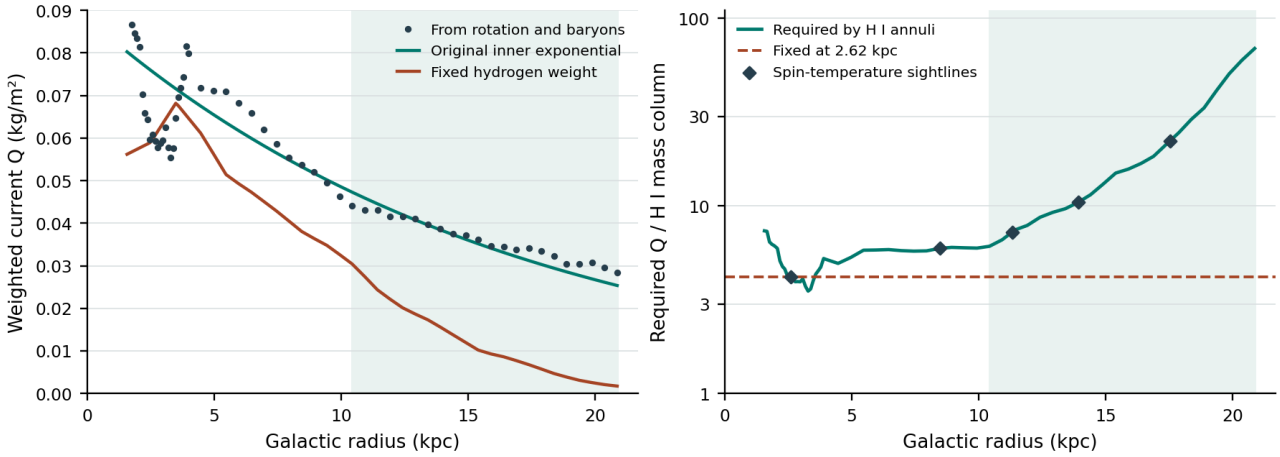

The shaded region is the outer half of the measured radius. Dots on the left are inferred from speeds and the baryonic model. Diamonds on the right mark radii with independent spin-temperature information. The gas-column prediction uses the single 2.62 kpc calibration. The near equality of the triplet/singlet entropy across these temperatures makes the ratio on the right effectively independent of its tiny temperature correction.

Speed, baryons and the explicit radial factor

The measured Q slope splits as **−1 + 0.162 + 0.187**. The −1 comes from the explicit 1/r. The other terms come from the variation of the observed squared speed and the decline in the modeled baryonic squared speed, respectively. The split uses exact adjacent differences in $\ln(v^2 - v_b^2)$, with the same log-radius fit for every term. It explains the observed kinematics conditional on the mass model.

Drawing independent speeds from their quoted uncertainties gives a conditional 95% slope range of −0.819 to −0.497. Varying the stellar disk mass-to-light ratio from 0.4 to 0.6 shifts the nominal slope from −0.682 to −0.618. These checks hold distance and inclination fixed. The reconstruction is a finite-disk measurement and leaves the behavior beyond 20.87 kpc open.

Original ESFD/SEFD equation guide §§8–10 · SPARC rotation and baryonic mass models · The numerical decomposition, noise draws and map-coverage checks are in the research files.

What the original entropy equation adds

The radio measure supplies an entropy **per area** if the neutral-hydrogen hyperfine states represent the SFD carrier. Let N be the face-on H I number column, $L = N/n$ its effective depth, and $S_A = N k_B h_{hf}$. Then $s = S_A/L$ and

$$Q_r/S_A = \beta_s J_r/(c^2 L).$$

At 2.62 kpc the annular column gives $S_A = \mathbf{163.7\ J\ K^{-1}\ m^{-2}}$ and $Q_r = \mathbf{0.06010\ kg\ m^{-2}}$. Their ratio is $\mathbf{3.67 \times 10^{-4}\ kg\ K/J}$. A single Gaussian with 1 kpc full width at half maximum would give a midplane s of 4.98×10^{-18} J K^{-1} m^{-3}. At 3 kpc width it would be 1.66×10^{-18}. Line-profile observations admit a thin disk plus a more slowly rotating thick component. Those illustrative single-layer conversions require a choice of which material carries the field.

A sign test inside SFD

For a regular center, the original stationary equation $\beta_s \nabla\cdot J = 2\gamma_s \nabla^2 s - U'(s)$ integrates to

$$c^2 Q_r = \gamma_s (s^2)' - (s/r^2) \int_0^r t^2\, U'(s(t))\, dt.$$

If the entropy potential is constant throughout the enclosed region, positive stiffness γ_s requires Q_r and $(s^2)'$ to have the same sign. For neutral hyperfine entropy in a layer of fixed or increasing effective depth, the outer gas profile makes $(s^2)'$ negative. **All 21 NGC 2403 outer points require positive Q_r.** All 99 covered outer rows in the ten primary dwarfs also require a positive source under the archive's fiducial baryonic disks, while their published smooth H I profiles decline. The best nonnegative constant-potential gradient coefficient fitted to NGC 2403's 38 inner gas-matched rows is zero.

For a general potential the same equation gives the volume average $\langle U' \rangle_{<r} = 6\gamma_s s'/r - 3c^2 Q_r/(rs)$. Positive Q_r, positive s and a negative s' require a **negative enclosed mean potential derivative** for positive stiffness. This condition can discriminate among proposed entropy potentials without choosing one from the rotation data.

The H I column itself has slope −4.121 across the 21 radii. The required $\beta_s J_r/L$ must therefore have slope +3.470 under this carrier assumption. Requiring 90% H I detection within each annulus shortens the span to 17.39 kpc and gives +2.429. Both estimates require the remaining factor to grow outward.

With a measured volume entropy profile and a specified U', the original equation would give $\gamma_s = [c^2 \nabla\cdot(Q_r \hat{r}/s) + U'(s)]/(2\nabla^2 s)$ wherever $\nabla^2 s$ is nonzero. Thus a measured thickness and independently constrained potential would make a radial consistency test for one constant γ_s possible. A calibrated J_r would then give β_s directly from the gravity equation.

Original stationary SFD entropy equation under the project's metric convention · Schaap, Sancisi & Swaters on NGC 2403's vertical gas structure · The sign test includes signed baryonic residuals in the archival sample.

Cancelling the unknown potential at equal entropy

NGC 2403's H I column rises from 6.38 to 7.79 solar masses/pc^2 between 1.5 and 3.5 kpc and declines on the far side of that peak. The same column therefore occurs at two different radii. If the layer has constant effective depth and saturated hyperfine entropy per atom, these two radii have the same volume entropy. They must have the same $U'(s)$ for any single-valued potential. Subtracting the original SFD equations at the two radii cancels U' exactly.

Let $x = r/(1\ \text{kpc})$, let f be the numerical H I mass column in solar masses/pc^2 and write $s = s_0 f$. Define $A = f'' + 2f'/x$ and $B = (Q/f)' + 2(Q/f)/x$, with primes here taken with respect to x. The original equations then give

$$K_\gamma \Delta A = \Delta B, \text{ with } K_\gamma = 2\gamma_s s_0^2/[c^2\ (1\ \text{kpc})].$$

The difference is between two radii with the same f. This constrains an entropy-stiffness combination independently of β_s and the shape of U. Its sign equals the sign of γ_s. Its magnitude still contains the volume-entropy normalization, hence the unknown layer depth.

What the measured inner peak gives

Five common columns span 6.8–7.6 solar masses/pc^2. Shape-preserving interpolation pairs radii of 2.60–3.21 kpc with 3.88–4.64 kpc. Rotation-inferred Q is averaged in the same 1 kpc rings. All five pairs share those measurements.

Interpolation of both profiles	Signed K_γ, kg/m^2	95% range from speed errors alone
Shape-preserving cubic	−0.000171	−0.000596 to +0.000240
Natural cubic	−0.000872	−0.002185 to +0.000405
Akima	−0.000199	−0.000658 to +0.000167

All nine combinations of gas and current interpolants prefer a negative signed coefficient. With $\gamma_s \geq 0$, every nominal fit lands at zero. Every conditional interval also includes positive values. The 1 kpc spacing limits the second radial derivative, and uncertainty in the volume entropy adds to the quoted intervals. A positive stiffness remains unresolved.

The same subtraction can be made *between* dwarfs at equal column if both share the same effective depth and potential. Thirty-nine of 45 pairs among the ten dwarfs have enough common coverage, giving 195 correlated comparisons. The nonnegative NGC fit predicts zero divergence difference. The unconstrained signed NGC value changes the mean pair discrepancy from 0.04864 to 0.04709 kg/m^2 and improves 24 of 39 pairs. This small change concerns the differentiated field equation. The next pages test the directly calibrated hydrogen weight against velocities.

Original SFD stationary equation §8 and gravity equation §9 · HALOGAS · LITTLE THINGS H I fits · The released code also recovers the known stiffness in a smooth example with a nonconstant potential.

One hydrogen weight carried to other galaxies

Define the dimensionless weight w by $Q_{trial} = w \Sigma_{HI} h_{hf}/\ln 4$, with the mass column in kg/m^2. The NGC 2403 sightline and rotation source at 2.62 kpc give **w = 4.19845**. Holding w fixed tests constant $\beta_s J_r/L$ across the disk and between galaxies. For disks with no measured spin temperature we use the saturated value ln 4. No target rotation speed enters this calibration.

Common coverage	Baryons alone, km/s	Original inner exponential, km/s	Fixed hydrogen weight, km/s
NGC 2403 outer, 21 rows	75.46	3.73	51.30
NGC 3198, 25 rows	50.44	5.74	13.98
NGC 5055, 14 rows	30.15	16.05	23.07
Ten dwarfs, 221 covered rows	17.05	22.71	12.70
Same dwarfs, 99 outer rows	21.38	26.05	11.70

Values are mean per-galaxy speed RMSE. The dwarf rows use the archive's fiducial baryonic disks and Hunter et al.'s H I fits inside the observed 90%-mass radius. Seven of ten dwarfs improve relative to baryons over the covered curves and eight improve over their covered outer halves. The paired outer improvement is 9.68 km/s, with a 95% galaxy-bootstrap range of 4.26–15.25 km/s. Across all covered radii the corresponding interval includes zero. Fitting w on all 38 gas-matched inner NGC 2403 rows gives 5.26245 and an outer dwarf error of 11.63 km/s. On NGC 2403 itself that alternative still gives 46.96 km/s.

Two additional sightlines measure atomic spin

Applying the same aperture convention to the 21-cm emission at each absorption position gives an independent check on the use of annular columns. The NGC 2403 calibration becomes w = 3.62 using the local, optically thin face-on column. At NGC 247's background absorption sightline (63 ± 15 K), it predicts 90.1 km/s against an interpolated 80.3. At dwarf NGC 2366's internal H II sightline (145 ± 60 K), it predicts 56.9 against 30.3 km/s. The latter is a weak, statistically integrated absorption detection. On this aperture convention the inferred local weights are 2.69 and 0.66 respectively. Optical depth, the fraction of emitting gas in front of a continuum source and spatial averaging limit this comparison.

Hunter et al., observed H I distributions and Table 2 · Oh et al., LITTLE THINGS rotation curves · Braun, individual H I sightlines.

Dwarf results with the observers' baryonic models

Oh et al. published the total and baryon-subtracted curves with separate radius and velocity normalizations. Undoing each normalization and matching actual radii recovers the authors' baryonic term $b = v_{total}^2 - v_{subtracted}^2$. On the 90 covered outer rows with a real baryon-only circular speed, **$w = 4.19845$ lowers mean error from 18.40 to 11.62 km/s**. It improves seven of ten dwarfs. The paired 95% interval for the mean reduction is 0.23–13.64 km/s, conditional on these ten galaxies.

Galaxy	Covered rows	Baryons alone, km/s	Fixed hydrogen weight, km/s
CVnIdwA	6	4.87	20.37
DDO 52	16	32.15	8.34
DDO 70	15	13.80	3.41
DDO 101	6	46.98	33.39
DDO 133	16	22.05	7.52
DDO 210	7	4.43	3.19
DDO 216	12	7.12	2.37
IC 1613	55	4.15	12.64
NGC 1569	24	3.85	21.86
UGC 8508	17	16.55	11.21

The table includes both inner and outer covered rows. The mean changes from 15.60 to 12.43 km/s over these 174 rows. CVnIdwA, IC 1613 and NGC 1569 worsen. The individual results show why a smaller average cannot establish a universal weight. Using the project's three gas-disk scale choices on identical rows gives outer hydrogen-model errors of 11.93, 12.05 and 12.21 km/s.

The published decomposition encodes the authors' modeled mass subtraction and shares rotation data with the total curve. Some residual velocities were unreported. Restoring six outer rows with a negative reconstructed baryonic force gives 96 rows for a squared-speed check. Mean RMSE falls from 1,095 to 826 $(km/s)^2$. Seven dwarfs already matched to the wider SPARC catalog and five additional Oh galaxies have separate scores. Among the five additional systems, two of five improve on covered curves and all four with outer coverage improve in ordinary speed.

Oh et al., published Data series in Figures 2–4, panels A and C · Hunter et al., Tables 1 and 2 · The archive includes the source tables, radius matches, signed force results and every galaxy's scores.

Does the slower exponential transfer without gas data?

The project also has **385 other galaxies** with rotation curves. On this larger set the original exponential $Q_r = C \exp(-r/r_s)$ can be tested using the known baryonic curve alone. Starting with $C = 0.08817$ kg/m^2, $r_s = 16.75$ kpc, keep the original Q at the 10.435 kpc calibration boundary. Matching NGC 2403's measured outer log slope sets **$C = 0.07342$ kg/m^2 and $r_s = 23.72$ kpc**. These two effective profile parameters are frozen for every target. NGC 2403's outer speeds helped choose this slope, so its own change from 3.73 to 3.16 km/s is a retrospective fit.

Transfer sample	Original → slower, whole curves	Original → slower, outer halves	Outer curves improved
130 other SPARC	31.38 → 28.23	37.06 → 32.35	104 of 130
245 PROBES	37.26 → 37.47	36.39 → 35.53	161 of 245
10 LITTLE THINGS dwarfs	23.67 → 20.81	26.74 → 23.38	9 of 10
255 external galaxies	36.73 → 36.82	36.01 → 35.05	170 of 255

All entries are mean per-galaxy RMSE in km/s. Every curve contributes on its own outer half, including short curves. The 255 external galaxies comprise PROBES plus the ten project dwarfs. The paired external outer reduction is 0.96 km/s, with a 95% interval of 0.70–1.23. On whole external curves the change is +0.09 km/s, with interval −0.10 to +0.28. On whole dwarf curves, baryons alone give 18.77 km/s. Changing the exponential length improves the original dwarf prediction while the hydrogen measurements supply more information where available. A finite exponential still declines faster than the 1/r current needed for a flat excess speed at arbitrarily large radius.

Which weight still needs an observation?

With equal triplet sublevels the mean projected spin is zero. If that isotropic gas alone supplies the spin tensor in the project's single-fluid axial current, it gives $J_r = 0$. The hydrogen-weight test uses the gas as a tracer of scalar entropy and asks how much directional current is still required. At fixed singlet/triplet ratio, exchanging the m = +1 and −1 populations of an oriented sample preserves its entropy and reverses its spin. Even for known s, the original equations allow $\beta_s \to a\beta_s$ and $J_r \to J_r/a$. Faraday rotation supplies a magnetic-field integral weighted by free-electron density. A calibrated measurement of the radial spin tensor in the source material and its effective depth would allow β_s to be inferred. The volume entropy profile and the response of its potential would independently test γ_s.

SPARC · PROBES public release · LITTLE THINGS · Heald et al., polarized radio and Faraday measurements.